

An in vitro evaluation of wettability and microbial adhesion of 316L stainless steel orthodontic archwires coated with Ag/PTFE nanoparticles

Avaliação *in vitro* da molhabilidade e da adesão microbiana de fios ortodônticos de aço inoxidável 316L revestidos com nanopartículas de Ag/PTFE

Mahmood Shakir NASER^{1,2} , Emad AL-HASSANI² , Fatima AL-HASSANI² 

1 - University of Kufa, Faculty of Engineering, Department of Materials Engineering. Najaf, Iraq.

2 - University of Technology, College of Materials Engineering. Baghdad, Iraq.

How to cite: Naser MS, Al-Hassani E, Al-Hassani F. An in vitro evaluation of wettability and microbial adhesion of 316L stainless steel orthodontic archwires coated with Ag/PTFE nanoparticles. Braz. Dent. Sci. 2026;29:e5032. <https://doi.org/10.4322/bds.2026.e5032>

ABSTRACT

Objective: This study investigated how silver/polytetrafluoroethylene (Ag/PTFE) nanoparticle coatings influence the surface wettability and bacterial adhesion of 316L stainless steel orthodontic archwires against *Streptococcus mutans* and *Staphylococcus aureus*. **Material and Methods:** Stainless steel archwires were ultrasonically cleaned, sterilized, and coated using RF sputtering. The coated surfaces were characterized using XRD and AFM; wettability and bacterial adhesion were analyzed using contact-angle measurements and microbial assays. **Results:** The Ag/PTFE coatings produced uniform, smooth layers, increasing the contact angle from 72.96° (uncoated) to 135.35° (30 min sputtering) and reducing roughness from 45 nm to 18 nm. Adhesion of *S. mutans* and *S. aureus* dropped to 1.54 and 2.16 CFU/mL, respectively. **Conclusion:** RF-sputtered Ag/PTFE coatings enhanced hydrophobicity and reduced bacterial adhesion, suggesting improved oral hygiene during orthodontic treatment.

KEYWORDS

Antiadherent; Nanoparticles; Radio frequency; Roughness; Wettability.

RESUMO

Objetivo: Este estudo investigou o efeito do revestimento com nanopartículas de prata/politetrafluoretileno (Ag/PTFE) na molhabilidade da superfície e na adesão bacteriana de fios ortodônticos de aço inoxidável 316L frente a *Streptococcus mutans* e *Staphylococcus aureus*. **Material e Métodos:** Fios ortodônticos de aço inoxidável (0,4 mm de diâmetro e 160 mm de comprimento) foram submetidos à limpeza ultrassônica, esterilizados e revestidos pelo método de *Sputtering* por radiofrequência (RF). O alvo de *Sputtering* foi composto por pós de prata (20 nm) e PTFE (25 nm) em escala nanométrica, compactados em um disco sólido. As características estruturais e morfológicas das superfícies revestidas foram analisadas por difração de raios X (XRD) e microscopia de força atômica em modo de flexão (AFM). A molhabilidade da superfície foi determinada por meio da medição do ângulo de contato, e a adesão bacteriana foi avaliada utilizando culturas de *S. mutans* e *S. aureus*. Os dados foram analisados por ANOVA de uma via, seguida pelo teste post hoc de Tukey (HSD), bem como por testes t para amostras independentes ($\alpha = 0,05$). **Resultados:** Os revestimentos de Ag/PTFE obtidos por *Sputtering* RF produziram uma superfície lisa e uniforme, com aumento significativo do ângulo de contato de 72,96° nos fios não revestidos para 135,35° após 30 minutos de deposição, indicando aumento expressivo da hidrofobicidade. A rugosidade superficial diminuiu de 45 nm para 18 nm, e a adesão bacteriana foi significativamente reduzida: *S. mutans* diminuiu de 350,8 UFC/mL para 1,54 UFC/mL, enquanto *S. aureus* reduziu de 223,6 UFC/mL para 2,16 UFC/mL após o revestimento. **Conclusão:** Os revestimentos de Ag/PTFE aplicados por *Sputtering* RF aumentaram significativamente a hidrofobicidade da superfície e reduziram a adesão bacteriana em fios ortodônticos de aço

inoxidável. Esses achados sugerem que o uso de revestimentos de Ag/PTFE pode contribuir para a redução da adesão bacteriana e da formação de biofilme em fios ortodônticos em condições *in vitro*.

PALAVRAS-CHAVE

Antiaderente; Nanopartículas; Radiofrequência; Rugosidade; Molhabilidade.

INTRODUCTION

The oral cavity harbors numerous microorganisms and provides a favorable environment for their proliferation. Among these, bacteria play a central role in enamel demineralization and periodontal infections. Enamel demineralization and periodontal infections are prevalent and concerning adverse consequences of orthodontic appliance treatment, occurring in roughly 50% of patients undergoing orthodontic therapy [1,2].

The issue becomes more pronounced when orthodontic wires are attached to the teeth via brackets that are adhered to either the labial or lingual surfaces of the teeth. As a result, maintaining effective oral hygiene becomes more challenging for patients. The typical progression of dental biofilm is enhanced by the attachment of dental plaque surrounding the brackets. Consequently, the likelihood of experiencing enamel decay or gingivitis, which can progress to periodontal disease, is a genuine concern [3].

Stainless steel archwires (SSW) have a high modulus of elasticity (stiffness) and high strength, making them very beneficial during the working stage of treatment. Moreover, they have the smoothest surface texture among the other types of archwires, are low-cost, exhibit low friction, possess good formability, demonstrate environmental stability, are biocompatible, and have good welding and soldering properties. These properties have contributed to the popularity of using stainless steel archwires since their introduction to the field of orthodontics [4,5]. The utilization of these devices results in increased retention of food particles and changes in the oral environment, including a reduction in pH, increased colonization by *Streptococcus mutans* (*S. mutans*) and *Staphylococcus aureus* (*S. aureus*), as well as the formation of biofilms and plaque buildup [6]. These alterations contribute to the formation of cavities and the demineralization of enamel, commonly referred to as white spot lesions, which are unattractive, detrimental to health, and potentially irreversible.

The major contributor involved in the formation of the biofilm that contributes to the progression of tooth decay is *S. mutans* [7].

One of the identified approaches for preventing and addressing dental lesions could involve the use of antimicrobial nanoparticles [8].

Nanoparticles are materials with dimensions typically ranging from 1 to 100 nm, characterized by unique physicochemical properties resulting from their high surface-to-volume ratio, that can be effectively integrated with dental materials or applied through surface coating techniques [9]. Various coating techniques and materials have been employed to enhance the surface properties of orthodontic appliances. Among the most widely used surface modification methods are electroplating, dip coating, sol-gel deposition, and chemical vapor deposition. However, these techniques often result in nonuniform coatings, high residual stresses, or require elevated temperatures that may alter the mechanical properties of orthodontic wires. In contrast, radio-frequency (RF) magnetron sputtering provides several advantages, including precise thickness control, strong film adhesion, low deposition temperature, and the ability to coat complex geometries uniformly. These advantages make RF sputtering particularly suitable for orthodontic applications, where maintaining the wire's mechanical integrity and achieving nanoscale homogeneity are critical. In the present study, this technique was selected to ensure a stable and uniform Ag/PTFE coating on stainless steel archwires, optimizing both surface smoothness and antibacterial functionality [10-13]. This technique involves removing surface atoms from a solid cathode (target) through bombardment with positive ions derived from an inert gas discharge, and subsequently depositing these surface atoms to create a thin film [14].

Recently, surface coatings utilizing metallic nanoparticles have been employed to enhance

the surface characteristics of orthodontic archwires. Metallic nanoparticles have become significant in surface coatings due to their enhanced characteristics at the nanoscale. Silver nanoparticles (Ag NPs) excel in surface coating applications due to their exceptional conductivity, catalytic properties, and well-documented chemical and physical characteristics, as well as their notable effectiveness against pathogens. Silver-based nanostructures have been incorporated into dental polymers [15] to modify functional performance while preserving biocompatibility, demonstrating that nanosilver-containing systems can tune physical behavior and still be considered for intraoral use [16]. The reason behind these characteristics is the high aspect ratio (surface-to-volume ratio) of Ag NPs, along with their low cost, non-cytotoxicity, and antibacterial action even at low concentrations [17,18].

The process of biofilm formation encompasses the early stages of bacterial adhesion, followed by bacterial growth and colonization, ultimately leading to the establishment of the biofilm. When the initial adhesion of bacteria to a surface is obstructed, the formation of biofilms will not occur. Polytetrafluoroethylene (PTFE) is recognized for its natural non-stick characteristics, which stem from its intrinsically low surface energy, fluorinated molecular structure, and pronounced hydrophobic behavior that reduce interfacial adhesion [19]. The integration of PTFE nanoparticles with Ag NPs through the RF sputtering technique leads to coatings exhibiting favorable characteristics, including resistance to bacteria, scaling, and corrosion [20,21]

The current study aimed to develop an anti-adhesive stainless steel archwire capable of minimizing microbial accumulation by depositing a thin layer of Ag/PTFE nanocomposite via RF sputtering. To the best of our knowledge, the use of Ag/PTFE nanolayers for orthodontic archwire coatings has not been previously reported.

MATERIALS AND METHODS

Materials

Nano-silver (Ag) powder (20 nm; purity > 99.95%; density 0.5 g/cm³) and nano-polytetrafluoroethylene (PTFE) powder (25 nm; purity > 99.95%; density 2.2 g/cm³) were obtained from Yujiang Chemical, China.

Stainless steel 316L archwires (Dentaurum, Germany) with a 0.4 mm round section, 160 mm length, and tensile strength between 2000 – 2300 N/mm² were used in this study.

Methods

Surface preparation

Foremost, the stainless-steel archwires (SSW) were ultrasonically cleaned in deionized water for 10 minutes using an ultrasonic bath operating at 40 kHz frequency and 60 W power (MTI Corporation, USA) to remove surface contaminants. Furthermore, the wires were dried and sterilized using ultraviolet light (Analytic, Germany) for 30 minutes prior to sputtering [22]. UV sterilization was selected to minimize potential thermal or moisture-induced alterations of the native stainless-steel surface prior to thin-film deposition, which could influence coating adhesion and nucleation behavior.

Target preparation and sputtering process

The sputtering target consisted of a compact Ag/PTFE disk obtained by thoroughly mixing the nanopowders and pressing them at 500 MPa (Figure 1). The target was mounted as the cathode, and the SSW was positioned as the anode at a distance of 60 mm in an RF magnetron sputtering chamber (Barez Afarin Industry, Iran). The chamber was maintained under a vacuum of 0.6×10^{-3} Pa, and high-purity argon gas was introduced at 0.6 Pa as the working atmosphere. During sputtering, the wires were continuously rotated to ensure uniform coating. Three sputtering durations of 10, 20, and 30 minutes were applied at a constant RF power of 60 W. Each experimental group consisted of five specimens (n = 5). The sample size was selected in accordance with specimen numbers commonly adopted in comparable in-vitro surface and microbial adhesion studies.

Characterization of coating layer

X-Ray Diffraction (XRD)

Phase composition and crystallinity of raw, coated, and uncoated samples were characterized using an X-ray diffractometer (Chongqing Drawell, China) equipped with a nickel filter and copper generator. The scanning speed was set



Figure 1 - Preparation steps of RF target.

to 6° per minute, and the diffraction angle (2θ) ranged from 10° to 80° .

Flex Atomic Force Microscopy (AFM)

The surface topography, nanoroughness, and particle size distribution of the coated and uncoated SSW were investigated using an interchangeable cantilever holder flex atomic force microscopy (AFM) (Nanosurf, Switzerland).

Wettability evaluation

Wettability of coated and uncoated samples was evaluated by the sessile-drop technique using an optical contact-angle meter (SL200KS, China). A $1 \mu\text{L}$ droplet of distilled water was placed on each surface, and the contact angle was recorded for 10 seconds. Each measurement was repeated three times, and the mean contact angle was calculated.

Antiadherent activity assessment

Bacterial strains used in this study included *Streptococcus mutans* and *Staphylococcus aureus*, clinical isolates identified using the VITEK® 2 automated microbial identification system (bioMérieux, France) prior to experimental procedures. For each strain, the microbial suspension was standardized to 0.5

McFarland ($\approx 1.5 \times 10^8$ CFU/mL) prior to use. Segments of coated and uncoated SSW were individually placed in test tubes containing 5 mL of artificial saliva prepared by dissolving K_2HPO_4 (0.2 g/L), KCl (1.2 g/L), KSCN (0.33 g/L), Na_2HPO_4 (0.26 g/L), NaCl (0.7 g/L), NaHCO_3 (1.5 g/L), and urea (0.13 g/L) in 1,000 mL of distilled water. The solution was filtered through $0.5 \mu\text{m}$ filter paper, and the pH was adjusted to 6.7 ± 0.1 using NaOH and lactic acid prior to use [23], then mixed with $100 \mu\text{L}$ of microbial suspension. The tubes were incubated at 37°C for 48 hours on an orbital shaker (Shimadzu, Kyoto, Japan). After incubation, each wire was rinsed in 5 mL phosphate-buffered saline (PBS) and shaken for 5 minutes at 2400 rpm (Heidolph, Germany) to detach weakly adhered bacteria. The resulting suspension was diluted $1000\times$ with PBS, and $100 \mu\text{L}$ from each dilution was spread on Mueller–Hinton agar plates and incubated at 37°C for 24 hours. Finally, the number of colony-forming units (CFU/mL) was determined [24,25].

Statistical analysis

Data obtained for contact angle and bacterial adhesion were analyzed using IBM SPSS Statistics (version 26). The normality of data was assessed

by the Shapiro–Wilk test ($p > 0.05$), confirming parametric distribution. Subsequently, a one-way analysis of variance (ANOVA) was employed to evaluate differences among the sputtering durations (0, 10, 20, and 30 minutes). When statistically significant differences were detected, pairwise comparisons were performed using Tukey's Honestly Significant Difference (HSD) post hoc test at a confidence level of 95%

($\alpha = 0.05$). The data are presented as mean \pm standard deviation (SD).

RESULTS

X-Ray Diffraction

Figure 2 shows the XRD patterns of both coated and uncoated stainless steel archwires (SSW). The uncoated SSW (Figure 2a) exhibits

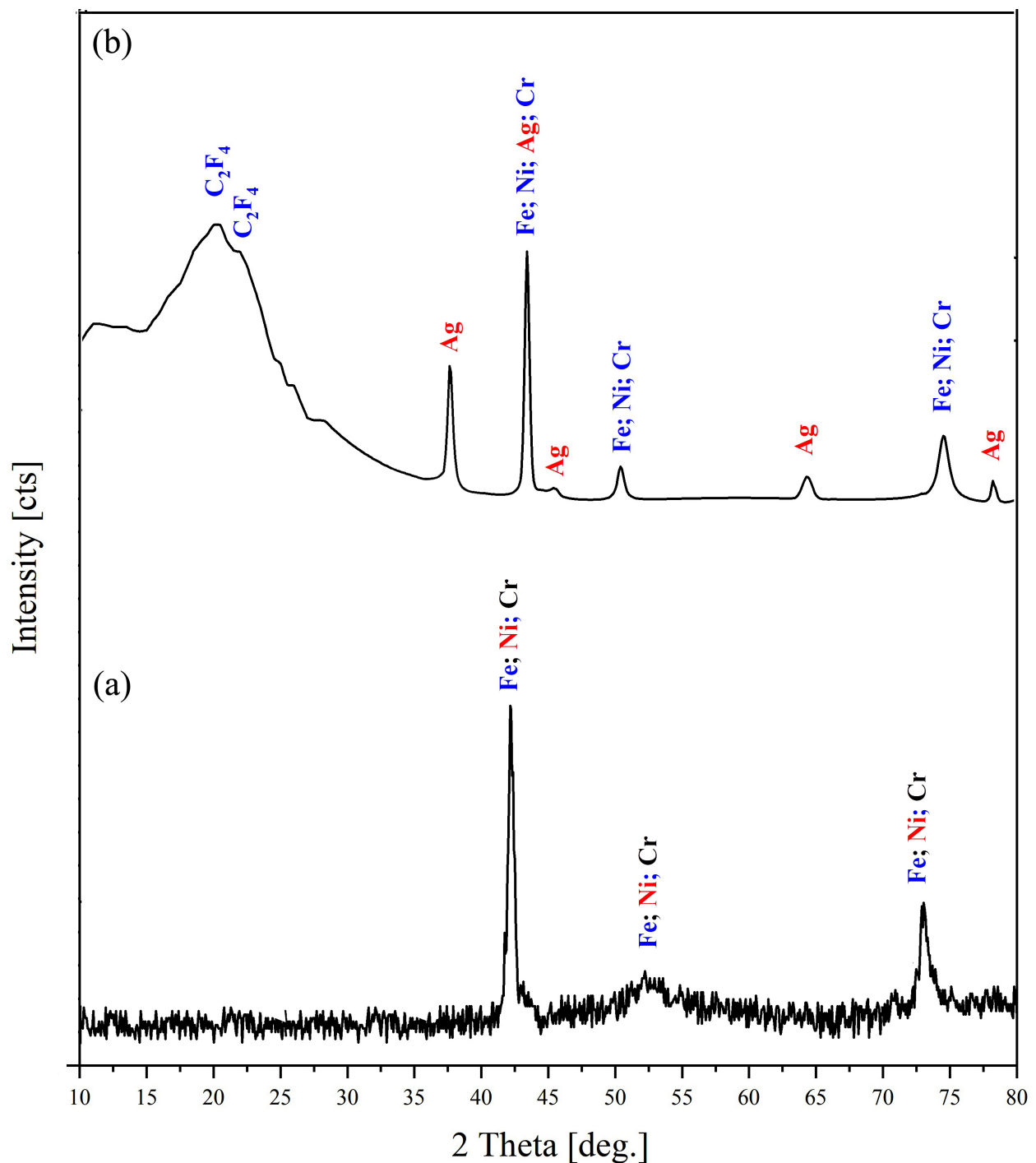


Figure 2 - XRD pattern of uncoated (a) and (b) Ag/PTFE coated SSW.

diffraction peaks corresponding to the primary austenitic γ -Fe cubic phase [26], whereas the coated Ag/PTFE SSW (Figure 2b) reveals diffraction peaks associated with both metallic silver and PTFE, forming a thin and continuous layer. Distinct diffraction peaks of silver appear at 2θ values of 37.6° , 44.0° , 64.4° , and 77.3° , which correspond to the (111), (200), (220), and (311) planes of the face-centered cubic (FCC) silver lattice. These peaks align well with the standard Joint Committee on Powder Diffraction Standards (JCPDS) card No. 04-0783 for cubic Ag nanoparticles [27]. Additionally, a broad peak at 21.2° corresponds to the polymeric PTFE phase, confirming the coexistence of both Ag and PTFE in the coating layer.

Flex Atomic Force Microscopy (AFM)

The surface morphology and roughness of the coated and uncoated SSW significantly influence coating adhesion [28]. Three-dimensional AFM images (Figure 3) demonstrate progressive changes in surface topology with increasing

sputtering time. As deposition time increased from 10 to 30 minutes, the color contrast in the AFM maps (brown and white zones) diminished, indicating smoother and more uniform surfaces. According to Table I, the mean surface roughness (Ra) of the uncoated SSW was 45 nm, which initially increased to 56 nm after 10 minutes of coating but subsequently decreased to 18 nm at 30 minutes, indicating a highly compact and smooth surface.

The corresponding nanoparticle size distribution histogram (Figure 4) shows a mean particle diameter of 53.75 nm, well within the nanoscale range (1–100 nm) [29]. These findings confirm that increasing sputtering time enhances coating uniformity and decreases surface irregularities, promoting better hydrophobic behavior [30].

Wettability

The contact-angle results, summarized in Table II and Figure 5, revealed a gradual increase

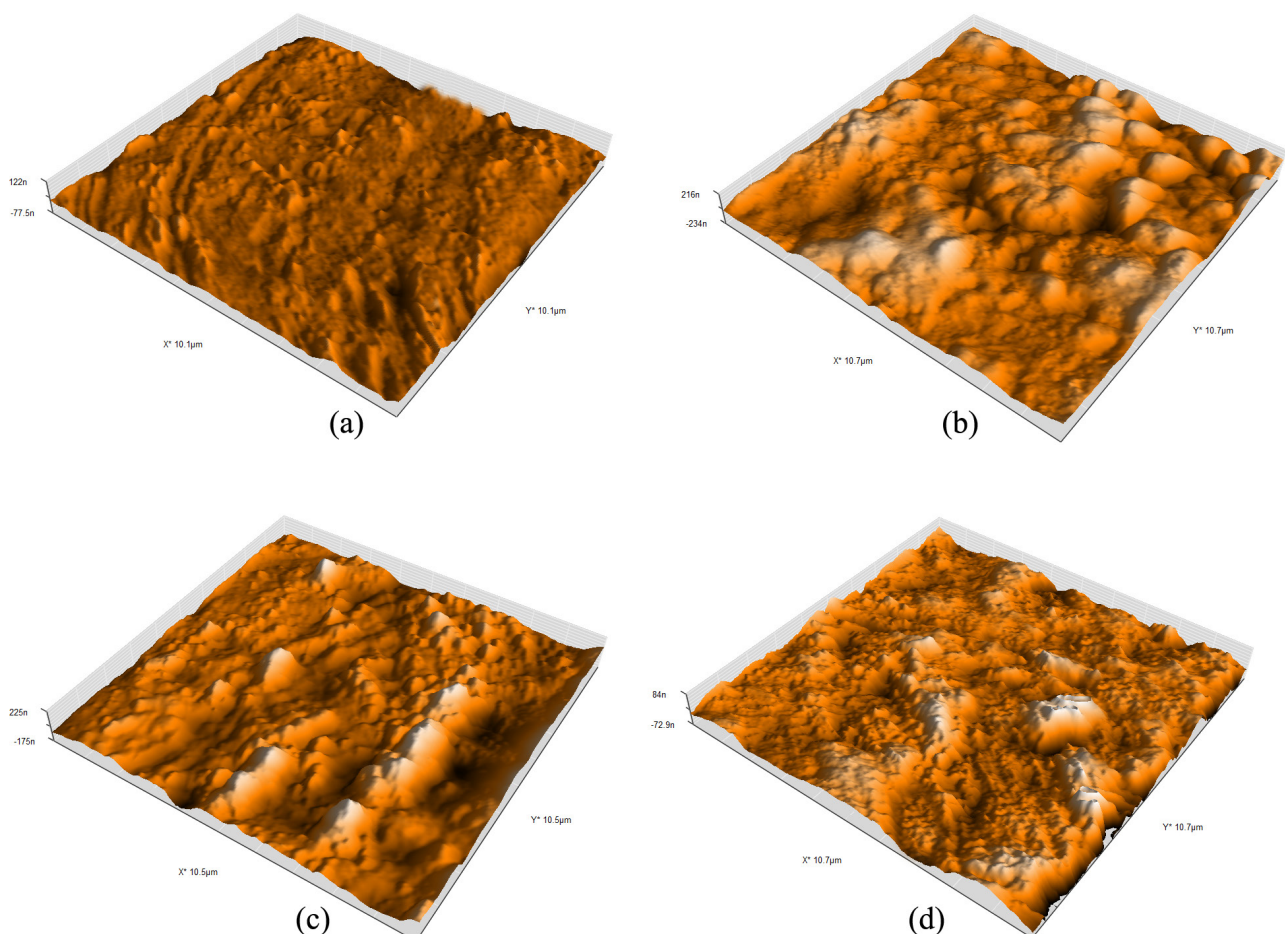


Figure 3 - Surface morphology of uncoated SSW(a) and Ag/PTFE coated SSW at different sputtering time (b) 10 min, (c) 20 min and (d) 30 min.

Table I - Average surface roughness of bared and Ag/PTFE coated SSW

Sample Symbol	Sample Condition	Sputtering Time (min)	Roughness Ra (nm)
SS	Bare SSW	0	45
A	Coated SSW	10	56
B	Coated SSW	20	32
C	Coated SSW	30	18

SS: uncoated stainless steel (control group); A: Ag/PTFE coating deposited for 10 minutes; B: Ag/PTFE coating deposited for 20 minutes; C: Ag/PTFE coating deposited for 30 minutes.

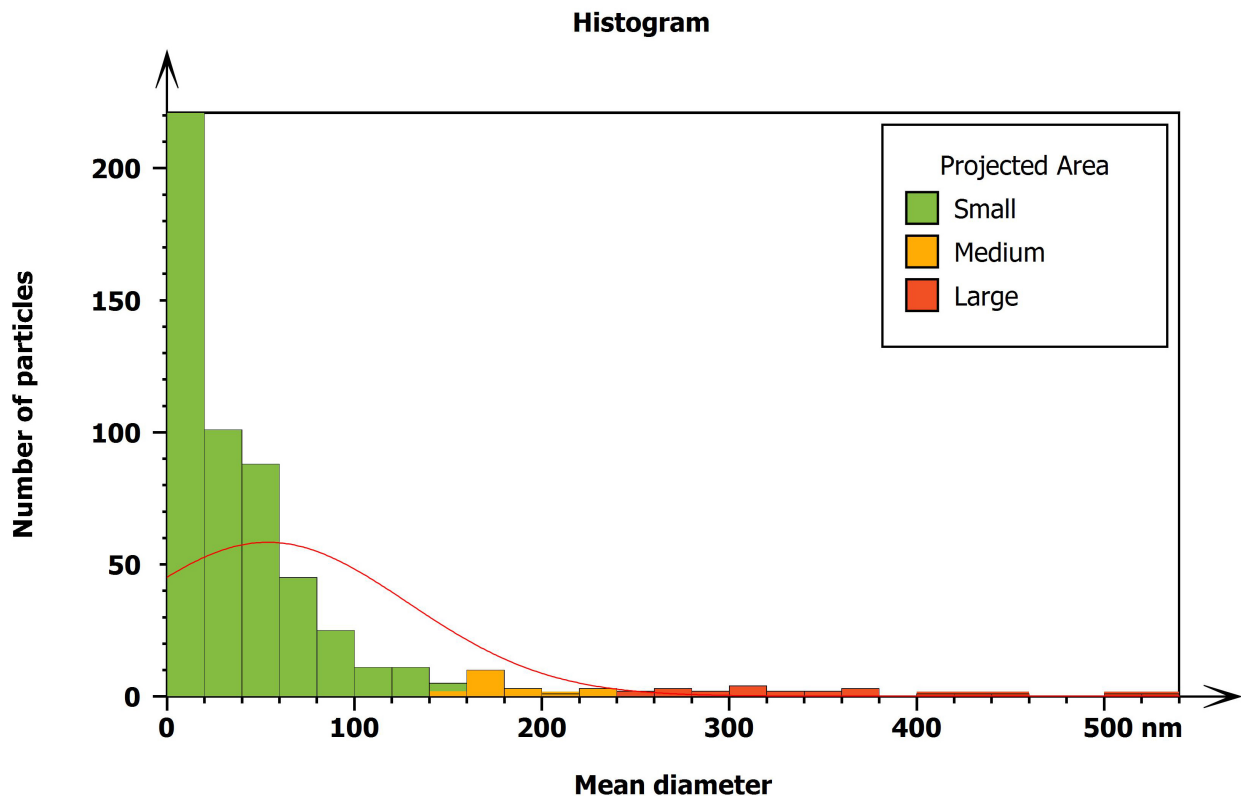


Figure 4 - Histogram for the Ag/PTFE nanoparticles coated on the SSW at 30 min explaining the percent of nanoparticles size and its distribution.

in hydrophobicity with longer sputtering durations. The mean contact angle (CA) of the uncoated SSW was 72.96° , corresponding to a hydrophilic surface. After 10 minutes of coating, the CA increased to 99.95° , and after 30 minutes it reached 135.35° , indicating a transition to a strongly hydrophobic surface. Normality was confirmed for all groups by the Shapiro–Wilk test ($p > 0.05$).

One-way ANOVA showed a significant effect of sputtering duration on contact angle (Table III; $p < 0.001$). Tukey's HSD post hoc comparisons (Table IV) indicated that each coated group differed significantly from the uncoated control ($p < 0.05$), with the 30-minute group presenting the highest hydrophobicity, as illustrated in Figure 6.

This progressive increase in contact angle demonstrates that the Ag/PTFE coating reduced the surface free energy of the SSW, thereby decreasing wettability and increasing hydrophobicity, in line with the physicochemical characteristics of PTFE and silver nanocomposites [31]. Based on the results obtained from the wettability and surface roughness analyses, the sample sputtered for 30 minutes (Group C) was selected for the microbial adhesion test. This group exhibited the most homogeneous and compact coating layer, along with the lowest surface roughness and the highest contact-angle value. Therefore, only the 30-minute group was advanced to microbiological evaluation to assess the antiadherent performance under the most optimized coating condition.

Table II - Mean contact angle ($^{\circ}$) of coated and uncoated stainless steel archwires

Group	Sputtering time (min)	Contact angle ($^{\circ} \pm$ SD)	p-value vs SS
SS (Control)	—	72.96 ± 2.84	—
A	10	99.95 ± 1.01	< 0.05
B	20	122.47 ± 1.37	< 0.05
C	30	135.35 ± 0.92	< 0.05

SS: uncoated stainless steel (control group); A: Ag/PTFE coating deposited for 10 minutes; B: Ag/PTFE coating deposited for 20 minutes; C: Ag/PTFE coating deposited for 30 minutes.

Table III - One-way ANOVA summary for contact angle among sputtering durations

Source	df	Mean square	F-value	p-value
Between groups	3	801.04	827.41	0.0000
Within groups	16	0.97	—	—
Total	19	2404.09	—	—

Note: One-way ANOVA indicated a significant effect of sputtering time on contact angle ($\alpha = 0.05$). Detailed ANOVA computations are presented in Table III.

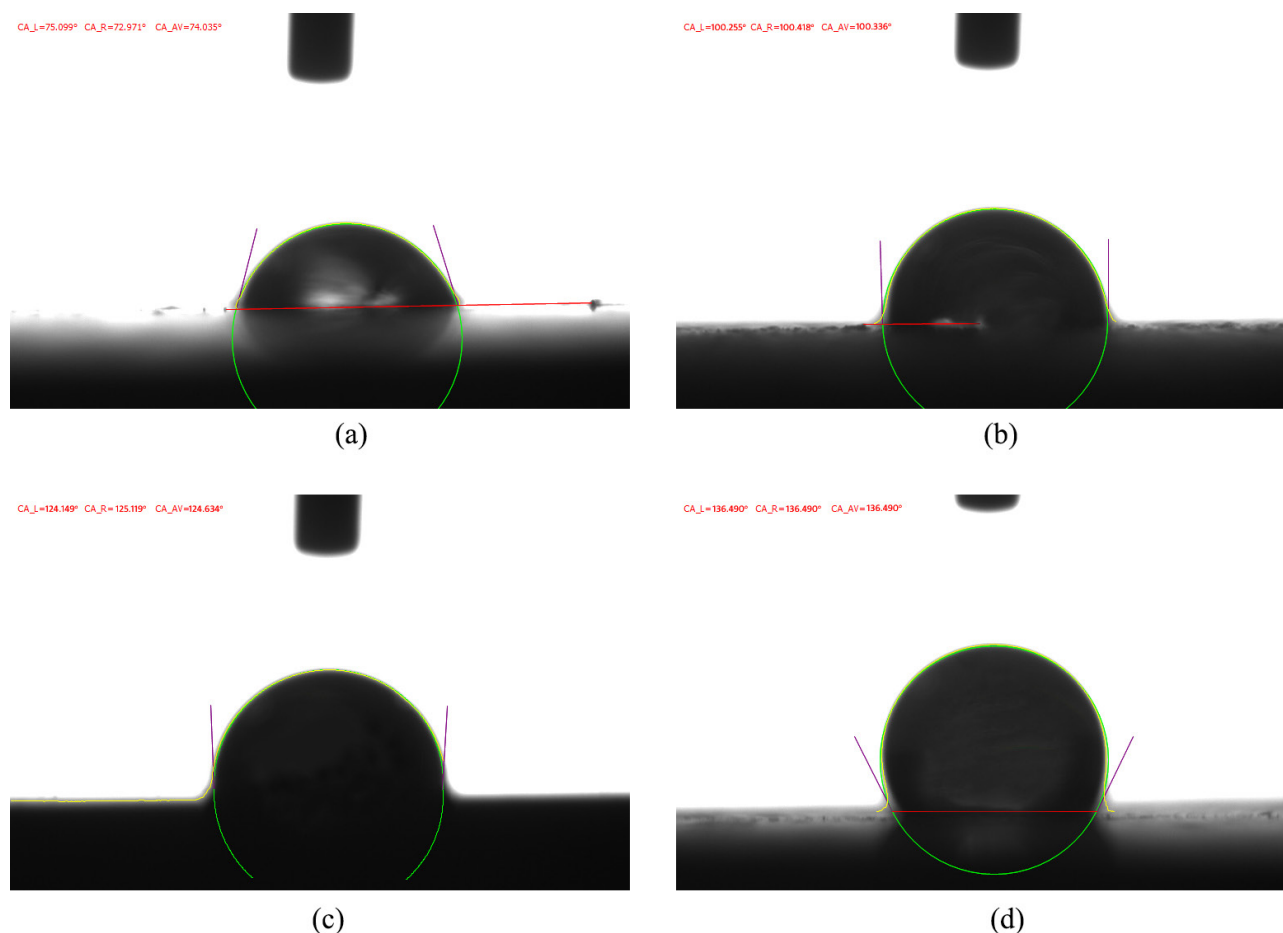


Figure 5 - Contact angle measurements for the uncoated SSW (a) and Ag/PTFE coated SSW at different sputtering time, (b) 10 min, (c) 20 min and (d) 30 min.

Antiadherent assessment

The antiadherent performance of the coatings against *S. mutans* and *S. aureus* is presented in Figure 7 and Table V. The uncoated control

samples (SS) showed high bacterial counts 350.8 CFU/mL for *S. mutans* and 223.6 CFU/mL for *S. aureus*. In contrast, the Ag/PTFE-coated samples sputtered for 30 minutes (sample C)

Table IV - Tukey's HSD post hoc comparisons for contact angle

Pairwise comparison	Mean difference (Δ°)	p-value	Interpretation
SS vs A	+27.0	< 0.05	Significant
SS vs B	+49.5	< 0.001	Significant
SS vs C	+62.4	< 0.001	Significant
A vs B	+22.5	< 0.01	Significant
B vs C	+12.9	< 0.05	Significant

SS: uncoated stainless steel (control group); A: Ag/PTFE coating deposited for 10 minutes; B: Ag/PTFE coating deposited for 20 minutes; C: Ag/PTFE coating deposited for 30 minutes.

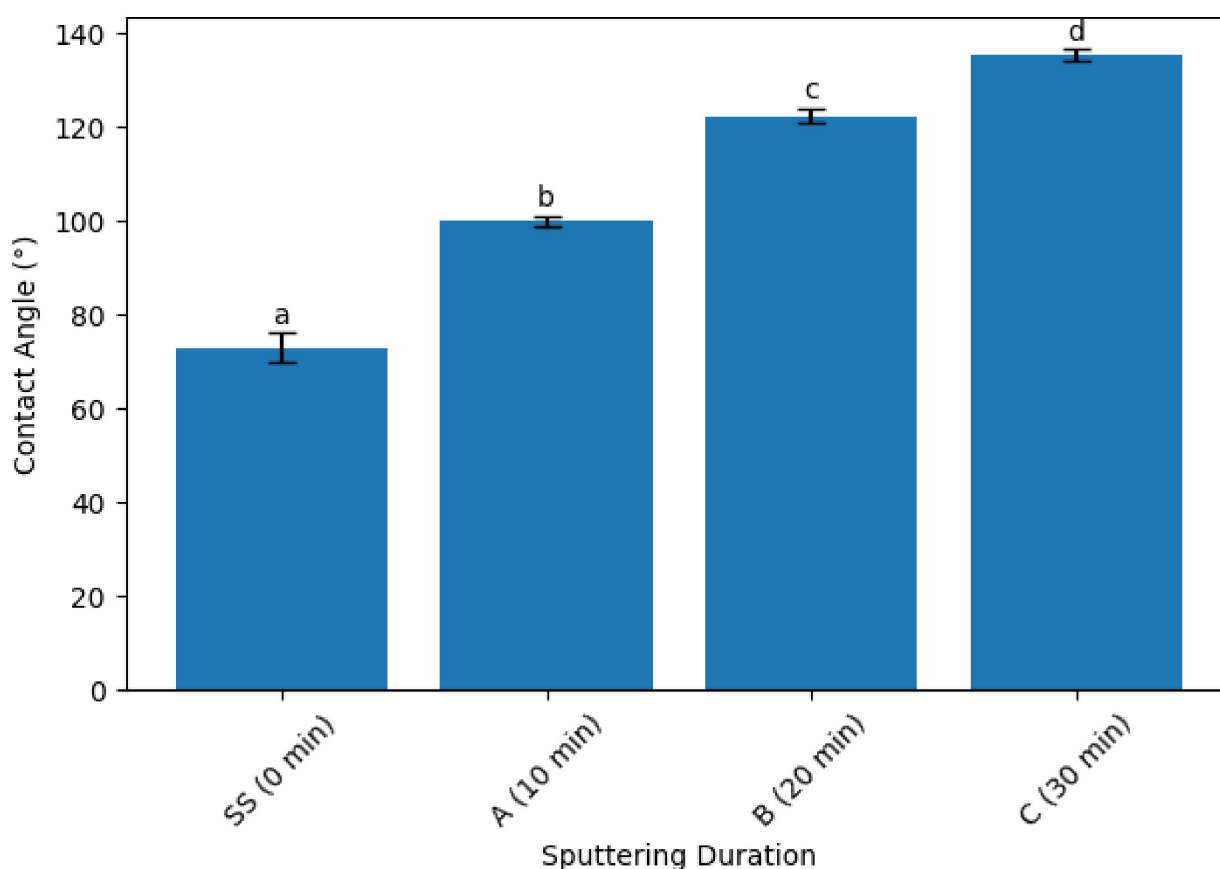


Figure 6 - Mean contact angle ($^\circ \pm$ SD) of uncoated and Ag/PTFE-coated stainless steel archwires at different sputtering durations. Different lowercase letters indicate statistically significant differences between groups (Tukey's HSD, $p < 0.05$).

exhibited a dramatic reduction in microbial adhesion, with mean values of only 1.54 CFU/mL and 2.16 CFU/mL, respectively.

Independent-sample t-tests demonstrated a statistically significant reduction in bacterial adhesion for both species ($p < 0.001$). These results confirm the strong antibacterial and antiadherent performance of the Ag/PTFE coating. The observed reduction in bacterial adhesion is attributed to both the bactericidal action of Ag NPs and the hydrophobic, low-energy surface of PTFE, which limits microbial attachment.

DISCUSSION

In this study, a uniform, hydrophobic, and antiadherent Ag/PTFE coating was successfully deposited on stainless steel orthodontic wires using RF magnetron sputtering. The XRD patterns confirmed the presence of Ag and PTFE phases covering the austenitic surface of stainless steel, while AFM images revealed the gradual transformation of the film from coarse clusters at 10 minutes to a smoother, more compact structure at 30 minutes. The decrease in roughness reflects the nucleation,

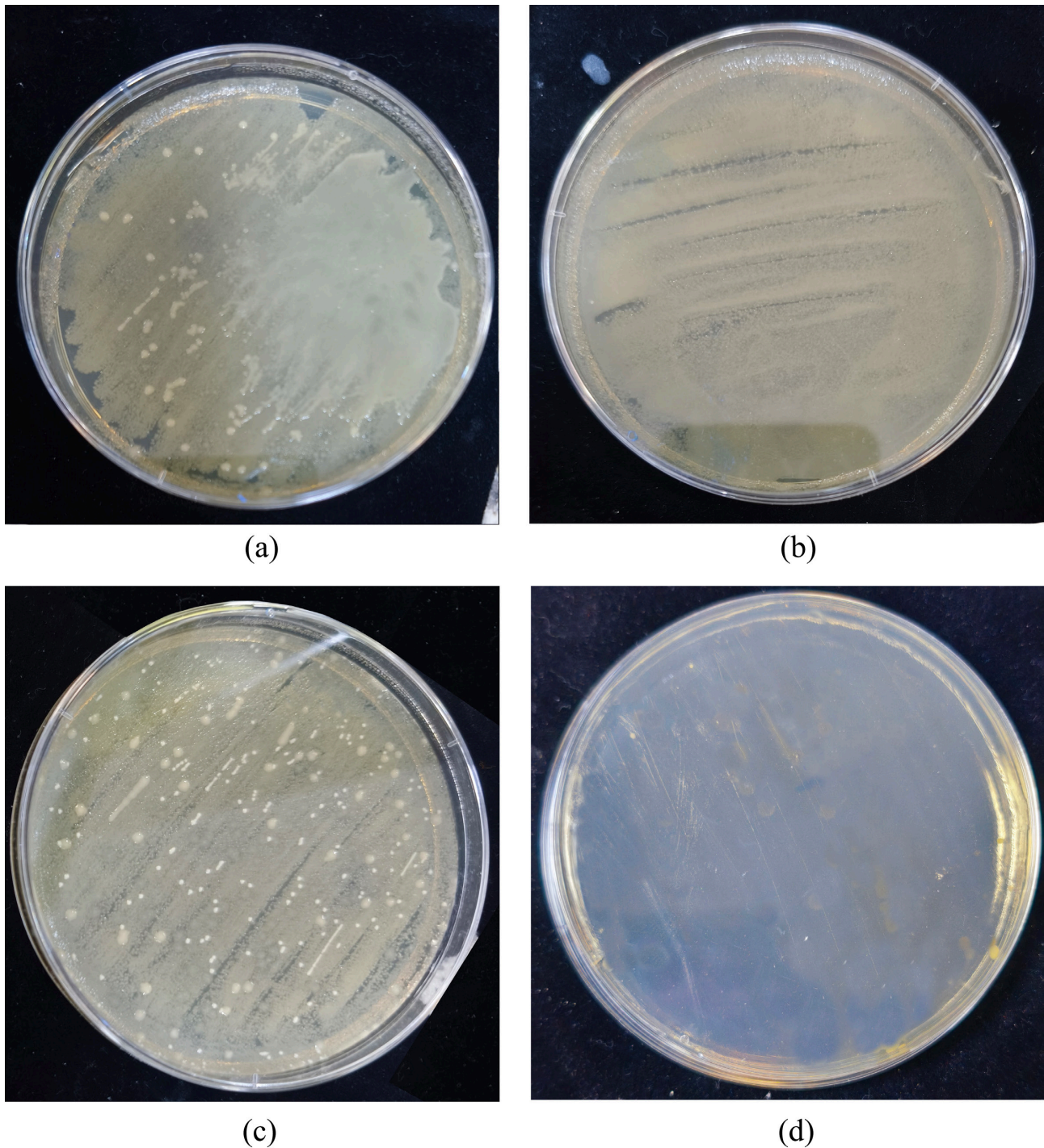


Figure 7 - Antiadherent assessment for *S. mutans* (a) uncoated SSW, (b) Ag/PTFE coated SSW at 30 min and *S. aureus* (c) uncoated SSW, (d) Ag/PTFE coated SSW at 30 min.

Table V - Bacterial adhesion (CFU/mL) on uncoated control (SS) and coated group (C, 30 min)

Microbial species	Group	Mean \pm SD (CFU/mL)	p-value
<i>Streptococcus mutans</i>	SS (Control)	350.8 \pm 37.5	—
	C (30 min)	1.54 \pm 0.37	< 0.001
<i>Staphylococcus aureus</i>	SS (Control)	223.6 \pm 18.9	—
	C (30 min)	2.16 \pm 0.67	< 0.001

Statistical comparisons between SS (control) and C (30 min) groups were performed using an independent samples t-test ($\alpha = 0.05$). Normality was confirmed using the Shapiro–Wilk test.

island growth, and coalescence phenomena that occur during thin-film formation via sputtering, leading to a denser and more uniform coating structure [32]. PTFE's low surface energy enables the formation of compact, continuous layers that minimize surface irregularities and limit bacterial attachment [33]. During the early stage of deposition, isolated Ag islands create temporary micro-protrusions, but prolonged sputtering connects these islands, reducing voids and creating a cohesive nanocomposite surface. This morphological refinement enhances both the mechanical adhesion of the coating and its biological compatibility [34,35]. In contrast, uncoated or rougher surfaces promote bacterial retention and biofilm growth due to increased surface area and microcavities [36]. The hydrophobicity of the coating increased progressively with sputtering time, reaching a contact angle of 135.35° at 30 minutes. This behavior may appear inconsistent with the Wenzel model [37], which associates higher roughness with stronger hydrophobicity, but can be better explained by the Cassie–Baxter regime [37], where air entrapment beneath the liquid droplet and the dominance of PTFE's chemical composition produce a high apparent contact angle even on smoother surfaces [38]. Our results align with those of Krishnan et al. [39], thus, in this study, surface chemistry particularly the PTFE component played a more decisive role than topography in defining wettability. Although surface roughness influenced the initial wetting regime, the dominant contribution of PTFE's intrinsically low surface energy appears to have governed both the observed increase in contact angle and the subsequent reduction in bacterial adhesion.

The antiadherent results strongly support the functional advantage of this nanocomposite. The substantial decrease in CFU counts for *S. mutans* and *S. aureus* ($p < 0.05$) can be attributed to a synergistic effect between Ag and PTFE, silver ions (Ag^+) disrupt bacterial membranes and inhibit polysaccharide synthesis, while PTFE's hydrophobic matrix prevents microbial attachment and biofilm formation. Similar antibacterial effects of nanosilver-based materials have also been confirmed by clinical studies in the oral environment [40,41].

The present findings demonstrate that combining Ag with PTFE can provide both bactericidal and antiadhesive effects without compromising the mechanical integrity of orthodontic wires. Nonetheless, as this is an

in vitro study, it does not account for intraoral variations such as pH, salivary enzymes, or mechanical wear. Furthermore, advanced surface chemical characterization techniques such as XPS or detailed elemental mapping could provide additional insight into the distribution and interaction of Ag and PTFE within the coating matrix. Future in vivo studies are necessary to evaluate the long-term durability, ion release, and biological safety of Ag/PTFE coatings under realistic clinical conditions [21,42].

CONCLUSION

In the present study, stainless steel orthodontic wires (SSW) were successfully coated with Ag/PTFE nanocomposites using the RF magnetron sputtering technique. Based on the findings, the following conclusions can be drawn:

1. The deposition of Ag and PTFE nanoparticles on the SSW surface was confirmed by XRD, indicating the successful formation of a uniform nanocomposite coating layer.
2. The sputtering time of 30 minutes produced the most uniform and homogeneous coating morphology, characterized by compact topography and stable particle distribution.
3. Increasing sputtering time resulted in a significant decrease in surface roughness from 45 nm (uncoated) to 18 nm—while simultaneously enhancing surface hydrophobicity (decreasing wettability), as reflected by the rise in water contact angle to 135.35°.
4. The Ag/PTFE coating exhibited strong antiadherent efficacy, reducing bacterial adhesion of *S. mutans* and *S. aureus* by more than 99%, thus demonstrating a marked reduction in biofilm-forming potential under in vitro conditions.

These findings indicate that Ag/PTFE nanocomposite coatings may contribute to reducing bacterial colonization and biofilm development on stainless steel orthodontic wires. However, further in vivo investigations are required to confirm their long-term clinical effectiveness and safety.

Acknowledgements

The authors thank the College of Materials Engineering, University of Technology, and the

Department of Materials Engineering, University of Kufa, for their technical support and laboratory facilities.

Data availability

All data supporting the findings of this study are available from the corresponding author upon reasonable request. No preprints or publicly archived datasets were used.

Author's Contributions

MSN: Conceptualization. EAH: Data Curation. FAH: Formal Analysis. EAH: Investigation. MSN: Methodology. EAH: Software. MSN: Supervision. EAH: Validation. FAH: Visualization. MSN: Writing – Original Draft Preparation. FAH: Writing – Review & Editing.

Conflict of Interest

No conflicts of interest declared concerning the publication of this article.

Funding

The authors declare that no financial support was received.

Regulatory Statement

This study did not involve human or animal participants and therefore did not require ethical approval.

REFERENCES

- Sundararaj D, Venkatachalapathy S, Tandon A, Pereira A. Critical evaluation of incidence and prevalence of white spot lesions during fixed orthodontic appliance treatment: A meta-analysis. *J Int Soc Prev Community Dent.* 2015;5(6):433-9. <https://doi.org/10.4103/2231-0762.167719>. PMID:26759794.
- Al-Blaihied D, El Meligy O, Baghlah K, Aljawi RA, Abudawood S, El Meligy OA. White spot lesions in fixed orthodontics: A literature review on etiology, prevention, and treatment. *Cureus.* 2024;16(7):e65679. <https://doi.org/10.7759/cureus.65679>. PMID:39205762.
- Gil FJ, Espinar-Escalona E, Clusellas N, Fernandez-Bozal J, Artes-Ribas M, Puigdollers A. New bactericide orthodontic archwire: NiTi with silver nanoparticles. *Metals.* 2020;10(6):702. <https://doi.org/10.3390/met10060702>.
- Littlewood SJ, Mitchell L. An introduction to orthodontics. 4th ed. Oxford: Oxford University Press; 2019.
- AlSubie M, Talic N. Variables affecting the frictional resistance to sliding in orthodontic brackets. *Dent Oral Craniofac Res.* 2016;2(3):271-5. <https://doi.org/10.15761/DOCR.1000160>.
- Tu Y, Ren H, He Y, Ying J, Chen Y. Interaction between microorganisms and dental material surfaces: general concepts and research progress. *J Oral Microbiol.* 2023;15(1):2196897. <https://doi.org/10.1080/20002297.2023.2196897>. PMID:37035450.
- Lemos JA, Palmer SR, Zeng L, Wen ZT, Kajfasz JK, Freires IA, et al. The biology of *Streptococcus mutans*. *Microbiol Spectr.* 2019;7(1):7.1.03. <https://doi.org/10.1128/microbiolspec.GPP3-0051-2018>. PMID:30657107.
- Sato TP, Conjo CI, Rossoni RD, Junqueira JC, Melo RM, Durán N, et al. Antimicrobial and mechanical acrylic resin properties with silver particles obtained from *Fusarium oxysporum*. *Braz Dent Sci.* 2018;21(1):96-103. <https://doi.org/10.14295/bds.2018.v21i1.1534>.
- Eker F, Duman H, Akdaşçi E, Bolat E, Saritaş S, Karav S, et al. A comprehensive review of nanoparticles: from classification to application and toxicity. *Molecules.* 2024;29(15):3482. <https://doi.org/10.3390/molecules29153482>. PMID:39124888.
- Jilani A, Abdel-wahab MS, Hammad AH. Advance deposition techniques for thin film and coating. London: Intech Open; 2017. <https://doi.org/10.5772/65702>.
- Zhang R, Han B, Liu X. Functional surface coatings on orthodontic appliances: reviews of friction reduction, antibacterial properties, and corrosion resistance. *Int J Mol Sci.* 2023;24(8):6919. <https://doi.org/10.3390/ijms24086919>. PMID:37108082.
- Borowski P, Myśliwiec J. Recent advances in magnetron sputtering: from fundamentals to industrial applications. *Coatings.* 2025;15(8):922. <https://doi.org/10.3390/coatings15080922>.
- Arango S, Peláez-Vargas A, García C. Coating and surface treatments on orthodontic metallic materials. *Coatings.* 2013;3(1):1-15. <https://doi.org/10.3390/coatings3010001>.
- Arici N, Akdeniz BS, Oz AA, Gencer Y, Tarakci M, Arici S. Effectiveness of medical coating materials in decreasing friction between orthodontic brackets and archwires. *Korean J Orthod.* 2021;51(4):270-81. <https://doi.org/10.4041/kjod.2021.51.4.270>. PMID:34275883.
- Hussain WS, Oleiwi JK, Hamad QA. Study of physical properties of biocomposite based on the polymer blends used for denture base applications. *Eng Technol J.* 2023;41(0):1474-87. <https://doi.org/10.30684/etj.2023.141437.1496>.
- Liao C, Li Y, Tjong SC. Bactericidal and cytotoxic properties of silver nanoparticles. *Int J Mol Sci.* 2019;20(2):449. <https://doi.org/10.3390/ijms20020449>. PMID:30669621.
- Alaloosi HA, Noori FTM, Jidran AK. The fundamental of reduced graphene oxide with nanosilver composite films using the spin coating technique. *Eng Technol J.* 2022;40(8):1023-8. <https://doi.org/10.30684/etj.v40i8.2205>.
- Abbas RH, Haleem AM, Judran AK. Fabrication of silver nanoparticles in aqueous solution by laser technique and study of their hemocompatibility and antibacterial effects against dental decay bacteria. *Eng Technol J.* 2023;41(4):543-52. <https://doi.org/10.30684/etj.2023.136922.1329>.
- Paz-Gómez G, del Caño-Ochoa JC, Rodríguez-Alabanda O, Romero PE, Cabrerizo-Vílchez M, Guerrero-Vaca G, et al. Water-repellent fluoropolymer-based coatings. *Coatings.* 2019;9(5):293. <https://doi.org/10.3390/coatings9050293>.
- Siegel J, Polívková M, Kasálková NS, Kolská Z, Svorčík V. Properties of silver nanostructure-coated PTFE and its biocompatibility. *Nanoscale Res Lett.* 2013;8(1):388. <https://doi.org/10.1186/1556-276X-8-388>. PMID:24044426.
- Zhang S, Wang L, Liang X, Vorstius J, Keatch R, Corner G, et al. Enhanced antibacterial and antiadhesive activities of Silver-PTFE nanocomposite coating for urinary catheters. *ACS Biomater Sci Eng.* 2019;5(6):2804-14. <https://doi.org/10.1021/acsbomaterials.9b00071>. PMID:33405585.

22. Soltanalipour M, Khalil-Allafi J, Mahdavi S, Etmianfar M. Boosting NiTi implant performance with crystalline Ta₂O₅: role of deposition rate and post-heat treatment. *J Mater Res Technol*. 2025;39:7051-64. <https://doi.org/10.1016/j.jmrt.2025.11.076>.
23. Mohammed SA, Mahmood AB, Al-Sheakli I. Measurement of surface roughness of copper nickel titanium arch wires at dry and wet conditions: An *In vitro* study. *J Res Med Dent Sci*. 2019;7(6):21-6.
24. Nafarrate-Valdez RA, Martínez-Martínez RE, Zaragoza-Contreras EA, Áyala-Herrera JL, Domínguez-Pérez RA, Reyes-López SY, et al. Anti-adherence and antimicrobial activities of silver nanoparticles against serotypes C and K of *Streptococcus mutans* on orthodontic appliances. *Medicina*. 2022;58(7):877. <https://doi.org/10.3390/medicina58070877>. PMID:35888596.
25. Fatene N, Mounaji K, Soukri A. Effect of eugenol on *Streptococcus mutans* adhesion on NiTi orthodontic wires: in vitro and in vivo conditions. *Eur J Gen Dent*. 2021;10(3):151-7. <https://doi.org/10.1055/s-0041-1736372>.
26. Abdullah HA, Anaee RA. Characteristics and morphological studies of nd doped titanium thin film coating on sS 316L by DC sputtering. *Diyala J Eng Sci*. 2022;15:22-30. <https://doi.org/10.24237/djes.2022.15303>.
27. Siddiqui T, Zia MK, Muaz M, Ahsan H, Khan FH. Synthesis and characterization of silver nanoparticles (AgNPs) using chemico-physical methods. *Ind J Chem Anal*. 2023;6(2):124-32. <https://doi.org/10.20885/ijca.vol6.iss2.art4>.
28. Wang J, Ai C, Yun X, Chen Z, He B. Effects of 3D roughness parameters of sandblasted surface on bond strength of HVOF sprayed WC-12Co coatings. *Coatings*. 2022;12(10):1451. <https://doi.org/10.3390/coatings12101451>.
29. Abiodun-Solanke I, Ajayi D, Arigbede A. Nanotechnology and its application in dentistry. *Ann Med Health Sci Res*. 2014;4(9 Suppl 3):S171-7. <https://doi.org/10.4103/2141-9248.141951>. PMID:25364585.
30. Sakthinathan S, Meenakshi GA, Vinothini S, Yu C-L, Chen C-L, Chiu T-W, et al. A review of thin-film growth, properties, applications, and future prospects. *Processes*. 2025;13(2):587. <https://doi.org/10.3390/pr13020587>.
31. Zhang S, Liang X, Gadd GM, Zhao Q. A sol-gel based silver nanoparticle/polytetrafluorethylene (AgNP/PTFE) coating with enhanced antibacterial and anti-corrosive properties. *Appl Surf Sci*. 2021;535:147675. <https://doi.org/10.1016/j.apsusc.2020.147675>.
32. Kaune G, Ruderer MA, Metwalli E, Wang W, Couet S, Schlage K, et al. In situ GISAXS study of gold film growth on conducting polymer films. *ACS Appl Mater Interfaces*. 2009;1(2):353-60. <https://doi.org/10.1021/am8000727>. PMID:20353223.
33. Akram W, Farhan Rafique A, Maqsood N, Khan A, Badshah S, Khan RU. Characterization of PTFE Film on 316L Stainless Steel Deposited through Spin Coating and Its Anticorrosion Performance in Multi Acidic Mediums. *Materials*. 2020;13(2):388. <https://doi.org/10.3390/ma13020388>. PMID:31947700.
34. Chhattani S, Shetty PC, Laxmikant SM, Ramachandra CS. In vitro assessment of photocatalytic titanium oxide surface-modified stainless steel and nickel titanium orthodontic wires for its antiadherent and antibacterial properties against *Streptococcus mutans*. *J Indian Orthod Soc*. 2014;48(2):82-7. <https://doi.org/10.1177/0974909820140202>.
35. Mousavi SM, Shamohammadi M, Moradi M, Hormozi E, Rakhshan V. Effects of cold chemical (glutaraldehyde) versus autoclaving sterilization on the rate of coating loss of aesthetic archwires: A double-blind randomized clinical trial. *Int Orthod*. 2020;18(2):380-8. <https://doi.org/10.1016/j.ortho.2019.12.003>. PMID:32037209.
36. Al Groosh DH, Bozec L, Pratten J, Hunt NP. The influence of surface roughness and surface dynamics on the attachment of Methicillin-Resistant *Staphylococcus aureus* onto orthodontic retainer materials. *Dent Mater J*. 2015;34(5):585-94. <https://doi.org/10.4012/dmj.2014-045>. PMID:26438981.
37. Quéré D. Wetting and roughness. *Annu Rev Mater Res*. 2008;38(1):71-99. <https://doi.org/10.1146/annurev.matsci.38.060407.132434>.
38. Ju Y, Ai L, Qi X, Li J, Song W. Review on Hydrophobic Thin Films Prepared Using Magnetron Sputtering Deposition. *Materials*. 2023;16(10):3764. <https://doi.org/10.3390/ma16103764>. PMID:37241391.
39. Krishnan M, Seema S, Tiwari B, Sharma HS, Londhe S, Arora V. Surface characterization of nickel titanium orthodontic arch wires. *Med J Armed Forces India*. 2015;71(Suppl 2):S340-5. <https://doi.org/10.1016/j.mjafi.2013.12.006>. PMID:26843749.
40. Aly KHA, Riad MI, Elezz AA. Success rate of silver nano-particles in comparison to silver diamine fluoride in management of deep carious lesions: a randomized controlled clinical trial. *Braz Dent Sci*. 2023;26(4):e3956. <https://doi.org/10.4322/bds.2023.e3956>.
41. Besinis A, Hadi SD, Le HR, Tredwin C, Handy RD. Antibacterial activity and biofilm inhibition by surface modified titanium alloy medical implants following application of silver, titanium dioxide and hydroxyapatite nanocoatings. *Nanotoxicology*. 2017;11(3):327-38. <https://doi.org/10.1080/17435390.2017.1299890>. PMID:28281851.
42. Tu Y, Ren H, He Y, Ying J, Chen Y. Interaction between microorganisms and dental material surfaces: general concepts and research progress. *J Oral Microbiol*. 2023;15(1):2196897. <https://doi.org/10.1080/20002297.2023.2196897>. PMID:37035450.

Mahmood Shakir Naser
(Corresponding address)

University of Kufa, Faculty of Engineering, Department of Materials Engineering, Najaf, Iraq.
Email: mahmoods.alammar@uokufa.edu.iq

Editor-in-chief: Sergio Eduardo de Paiva Gonçalves

Editor: Bruno Mello de Matos

Date submitted: 2025 Oct 19

Accept submission: 2026 Mar 17